SUPPLEMENTARY MATERIALS

Supplementary Methods

RNA in situ hybridization

RNA in situ hybridization (ISH) was conducted using single-color chromogenic RNAscope assay (Advanced Cell Diagnostics Inc.). Pairs of oligonucleotide probes undergo sequence-specific hybridization for target-specific single-molecule detection. The probe used for human DLL3 was RNAscope LS 2.5 Probe-Hs-DLL3 (catalog no. 411338) and the probe for mouse DLL3 was Mus musculus delta-like 3 (Drosophila) (Dll3) mRNA (catalog no. 464268). RNA ISH staining of slides was performed on the Leica Bond III automated stainer (Leica Biosystems Inc.). Hybridization signals were detected under bright-field microscope as brown colorimetric staining, followed by counterstaining with hematoxylin. Signals were granular and discrete red dots that corresponded to individual RNA targets. Controls used for each DLL3 RNA ISH experiment were (i) RNAscope 2.5 LS Positive Control Probe Hs-PPIB (catalog no. 313908), and (ii) B. subtilis gene dihydrodipicolinate reductase (negative control, catalog no, 312038). The HALO software (Indica Labs Inc.) was used for automated image quantification of DLL3 RNA in situ expression at a single-cell resolution. Visual scoring is performed by a qualified scientist to assign a single score to a sample based on the predominant staining pattern throughout the entire sample.

Determination of kinetics and affinity of anti-DLL3 antibodies toward DLL3

The binding kinetics and affinity of various anti-DLL3 antibodies were determined at 37°C as both full-length monoclonal antibodies (IgG) and scFvs toward human, cynomolgus monkey (cyno) and mouse DLL3. For the scFvs, the variable regions of the anti-DLL3 antibodies derived from their respective hybridoma were cloned flanking a $(GGGGS)_3$ or $(GGGGS)_4$ linker followed by part of the hinge and Fc from a modified human IgG2 sequence resulting in a scFv-Fc fusion which was expressed using Expi293. The extracellular domain (ECD) from human, cyno and mouse DLL3 was fused with a C-terminal 8×His epitope tag and Avi tag, expressed using Expi293 then purified by immobilized metal affinity chromatography (IMAC) followed by size exclusion chromatography (SEC).

The antibody binding kinetics were determined by surface plasmon resonance (BiacoreTM surface plasmon resonance (SPR) system, GE Healthcare Bio-Sciences, Pittsburg PA). The antibodies diluted in HBS-T+ running buffer (0.01 M HEPES pH 7.4, 0.15 M NaCl, 0.05% v/v Tween20, 1 mg/mL BSA) were captured on a CM4 chip immobilized with an antibody specific for the anti-DLL3 antibody constant domains. Purified DLL3 was serially diluted into HBS-T+, injected for 2 min at 30 uL/min and a dissociation time of 10 min then the surface regenerated with either 10 mM Glycine-HCl pH 1.7 or phosphoric acid between injections. Kinetic association rates (kon) and dissociation rates (koff) are obtained simultaneously by fitting the data globally to a 1:1 Langmuir binding model (Karlsson, R. Roos, H. Fagerstam, L. Petersson, B. (1994). Methods Enzymology 6. 99-110) using the BIAevaluation program. Equilibrium dissociation constant (K_d) values are calculated as k_{off}/k_{on}.

Epitope mapping of DLL3 targeting antibodies

A panel of CHO cells expressing full length and a variety of truncated human DLL3 were used to determine which domain each DLL3 targeting antibody recognized. The extracellular domain of human DLL3 can be subdivided into different sub-domains that are defined by the following amino acid positions: Signal peptide: 1-26; N-terminus (N-ter): 27-175; DSL: 176-215; EGF1:215-249; EGF2:274-310; EGF3:312-351; EGF4:353-389; EGF5: 391-427; and EGF6: 429-465.

CHO cells expressing full length and truncated DLL3 (DSL-EGF6, EGF1-EGF6, EGF2-EGF6, EGF3-EGF6, EGF4-EGF6, EGF5-EGF6) with N-terminal HA tag were stained with hybridoma supernatant or purified DLL3 antibodies in PBS+1%BSA. Bound DLL3 antibodies were detected with PE labeled anti-mouse IgG antibody (Biolegend). Flow cytometry analysis demonstrated that, for example, if a clone binds to all truncated proteins including EGF3 but not to any truncated protein without EGF3, then such clone recognizes EGF3.

Disassociation of and T cell activation by primary human pancreatic cells

5x5x5 cm^3 samples from whole human pancreas were sourced from National Disease Research Interchange (NDRI) following proper corporate compliance and approval including agreement

that use of human tissue is authorized and universal precautions will be strictly followed. Specimen was placed in a rigid specimen container and filled with RPMI + 10% FBS and Penicillin/Streptomycin, stored at 2-8 ^{o}C until shipment. Upon arrival, specimen was removed from the container and into a petri dish with fresh RPMI + 10% FBS. Fat and connective tissue were carefully removed prior to dividing the sample into 500 mg cross-sections. Each 500 mg tissue piece was placed in a C-tube with 2.5 mL of the enzyme mix defined in the dissociation of inflamed neural tissue using Miltenyi Biotec Multi Tissue Digestion Kit #1 (Cat#130-110-201). Enzyme R was titrated down to 50% of published recipe concentration to support higher cell viability in product. Tissues in the C-tubes were digested on gentleMACS Octo Dissociator with heaters using gentleMACS Program 37C_Multi_F. After digestion, tissues were washed with cold D-PBS and strained (70 µm filter) into a new 50 mL conical tube. Samples were then washed and spun down at 300xg for 10min at 4 ^{o}C. Cells were resuspended in RPMI + 10% FBS.and plated at 1x10^{4} cells per well in 96-well plate. For controls, DLL3-positive DMS 273 and DLL3-negative U87 were plated at the same densities. DLL3 CAR Ts were added at E:T = 6:1 and 2:1 and co-cultured with targets for 2 days. At the end of 2 day co-culture, T cells were stained for activation markers (41BB and CD25) for analysis by flow cytometry.

Preparation and in vitro cytotoxicity of dissociated mouse pituitary cells

Mouse pituitaries from NSG mice were harvested under aseptic conditions and dissociated by 3 rounds of incubations at 37C in 1 mL dissociation mix [5 mL DMEM, high glucose, GlutaMax (Gibco), 50 uL Enzyme H, 5 uL Enzyme R, 6.25 uL Enzyme A (Miltenyi tumor dissociation kit)] followed by mechanical dissociation using trituration. Single cells were transferred to complete medium (DMEM, high glucose, GlutaMax, 20%, 1X Insulin-Transferrin-Selenium Solution, 1X MEM Non-Essential Amino Acids, 1X Penicillin-Streptomycin) and pooled following each round. Single cells were plated in 96-well plate in complete medium at 5x10^{4} cells per well and let to recover for 3 days before CAR T cells were added. At the time CAR T cells were added, the expected target density was 1x10^{4} cells per well. For controls, DLL3 positive DMS 273 and DLL3-negative 293T were plated at the same densities. DLL3 CAR Ts were added at E:T = 9:1, 3:1, and 1:1 and co-cultured with targets for 3 days. At the end of 3 day co-culture, the media was separated from the wells and centrifuged to pellet out the T cells. The

target cells were used for cytotox readout with CellTiter Glo (Promega). The T cells were pooled and stained for activation markers (41BB and CD25) for analysis by flow cytometry. The supernatant was frozen at -80C and then thawed for cytokine analysis using Human TH1/TH2 10-Plex Tissue Culture Kit (Meso Scale Discovery).

Mouse safety study using animals bearing intracranial tumors

LN229-vIII-mDLL3 cells in RPMI were injected intracranially in NSG mice ($3x10^4$ cells in 3 µL per mouse). Tumor growth was monitored by bioluminescent imaging. Two weeks post-implantation mice were assigned to groups such that each group had similar mean ±SD BLI signal. Non-transduced T cells, mouse cross-reactive DLL3 CAR-T cells and EGFRvIII CAR-T cells were thawed and injected at $1x10^7$ CAR+ cells/ mouse in 200uL by tail vein IV injection. In order to support CAR-T cell expansion and persistence, 0.5 ug IL-15 (Peprotech AF-200-15) and 3ug IL-15Ra Fc protein (R&D Systems 7194-IR) were given to each animal twice weekly ip starting on day 17 until the end of the study. Tumors continued to be monitored every 3-4 days until the end of the study. On days 22 and 38, brain and pituitary tissues from all animals fixed and stained with H&E or immunohistochemically stained to demonstrate hCD45 (Cell Signaling Technologies, clone D9M8I).

Immunohistochemistry

Formalin-fixed paraffin-embedded (FFPE) sections of mouse tissues were stained for CD3, CD45, ADH or oxytocin. Sections were blocked with Background Punisher (BioCare medical, Richmond CA) for 1 hour at RT and then incubated with anti-CD3 (Abcam, clone EP449E, dilution 1:500) or anti-CD45 (Cell Signaling Technologies, clone D9M8I, dilution 1:200) antibodies overnight at 4 °C, or with anti-ADH antibody (Immunostar, #20069, dilution 1:7000) for 15 minutes at RT, or with anti-oxytocin antibody (Immunostar, #20068, dilution 1:10000) for 1 hour at RT. Tissues were washed for 10 minutes with PBS+0.01% Tween-20 and incubated with Rabbit-on-rodent HRP-Polymer (Biocare Medical, RMR622) for 30 minutes at RT. Sections were next developed with DAB substrate kit (Vector laboratories) until signal appeared. Finally, sections were stained with Hematoxylin QS Counterstain (Vector laboratories, H-3404-

100), air dried and coverslipped.

Fig. S1

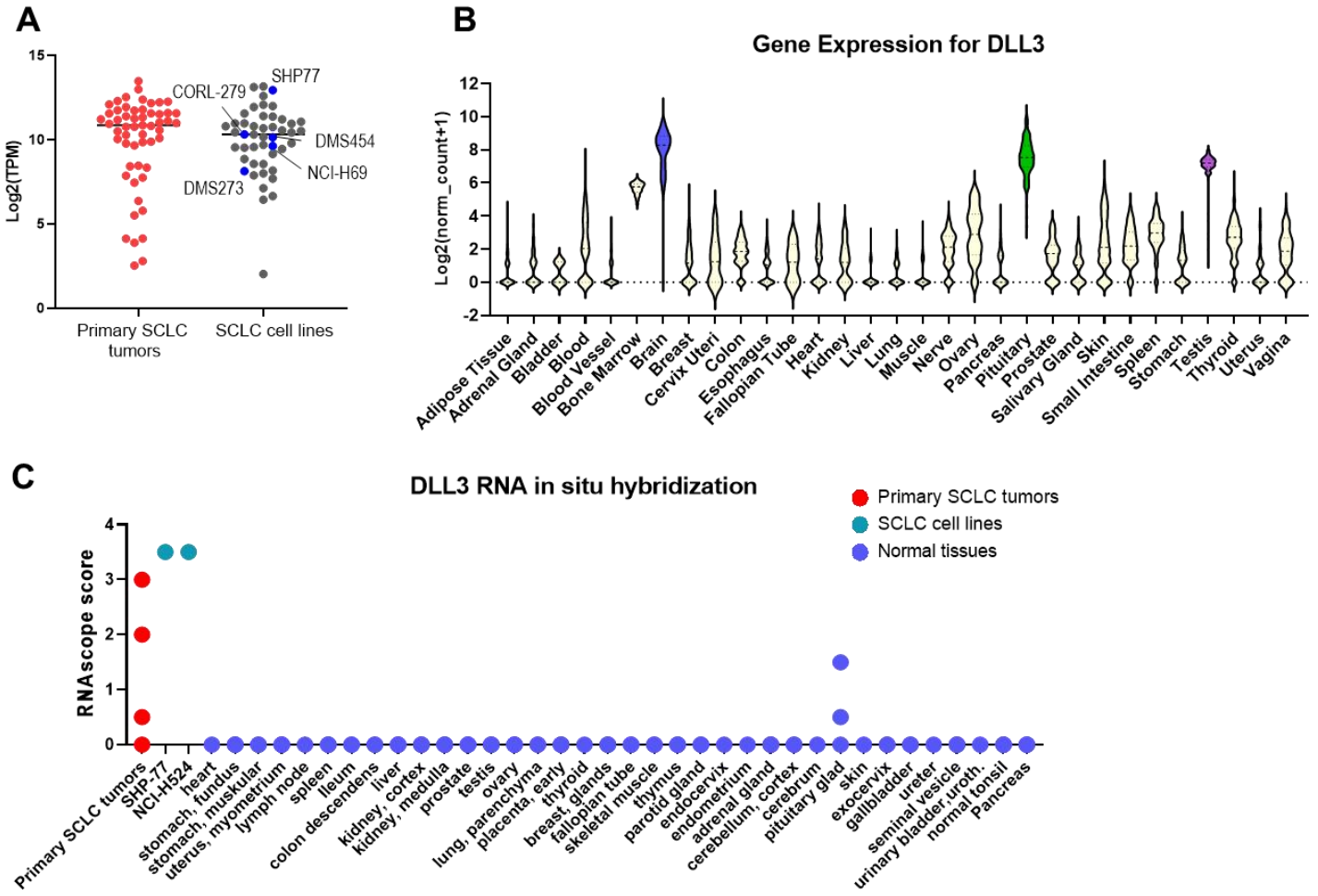
A
Log2(TPM)
CORL-279
SHP77
DMS454
NCI-H69
DMS273
Primary SCLC tumors
SCLC cell lines
B
Gene Expression for DLL3
Log2(norm_count+1)
Adipose Tissue
Adrenal Gland
Bladder
Blood
Blood Vessel
Bone Marrow
Brain
Breast
Cervix Uteri
Colon
Esophagus
Fallopian Tube
Heart
Kidney
Liver
Lung
Muscle
Nerve
Ovary
Pancreas
Pituitary
Prostate
Salivary Gland
Skin
Small Intestine
Spleen
Stomach
Testis
Thyroid
Uterus
Vagina
C
DLL3 RNA in situ hybridization
Primary SCLC tumors
SCLC cell lines
Normal tissues
RNAscope score
Primary SCLC tumors
SHP-77
NCI-H524
heart
stomach, fundus
stomach, muskular
uterus, myometrium
lymph node
spleen
ileum
colon descendens
liver
kidney, cortex
kidney, medulla
prostate
testis
ovary
lung, parenchyma
placenta, early
thyroid
breast, glands
fallopian tube
skeletal muscle
thymus
parotid gland
endocervix
endometrium
adrenal gland
cerebellum, cortex
cerebrum
pituitary glad
skin
exocervix
gallbladder
ureter
seminal vesicle
urinary bladder uroth.
normal tonsil
Pancreas

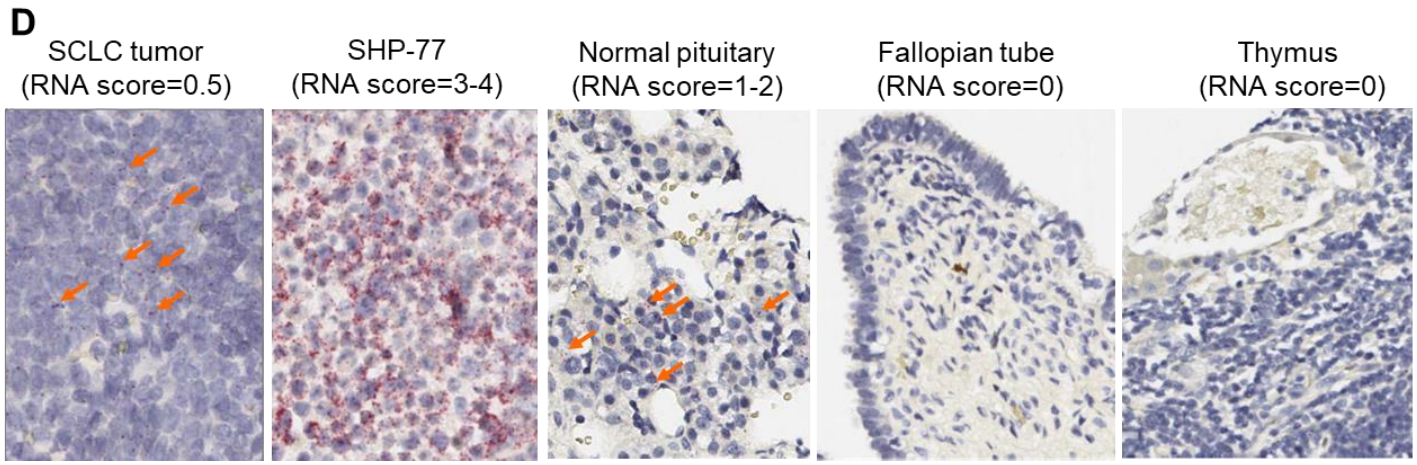
D
SCLC tumor
(RNA score=0.5)
SHP-77
(RNA score=3-4)
Normal pituitary
(RNA score=1-2)
Fallopian tube
(RNA score=0)
Thymus
(RNA score=0)

Fig. S1 continued

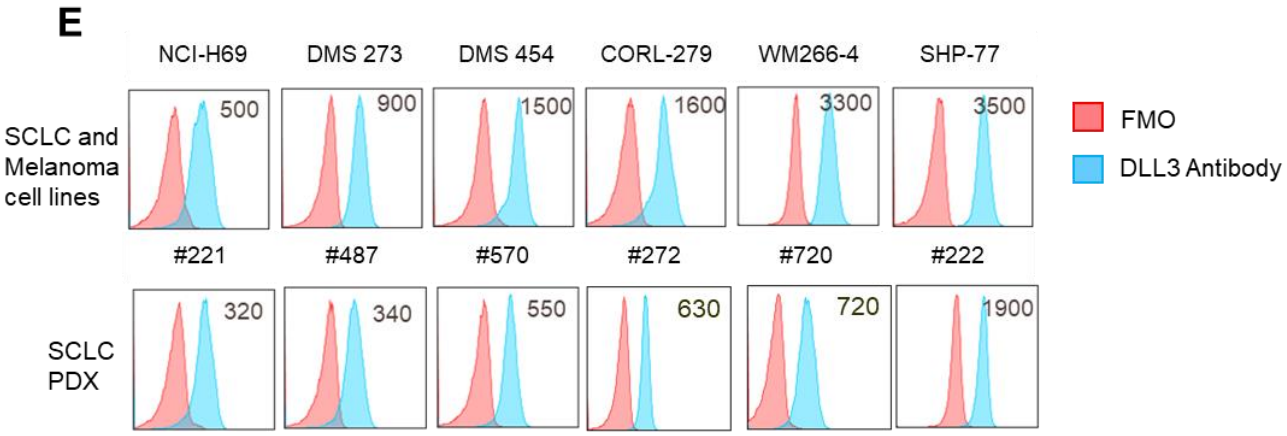

Fig. S1 DLL3 is expressed in small cell lung tumors, PDX models and cell lines, with limited expression in normal tissue. (**A**) DLL3 RNA analysis of primary SCLC tumors (n=55) and cell lines (n=47). TPM, transcripts per kilobase million. (**B**) mRNA expression of DLL3 in normal tissues according to GTEx RNASeq data (GTEx ENSG00000090932.10). TPM, transcripts per kilobase million. (**C**) RNA in situ hybridization analysis with probe specific for DLL3 shows DLL3 is expressed in SCLC tumors and cell lines. No expression was detected in normal tissues except brain, pituitary gland and testis. (**D**) Representative images of human DLL3 RNA in situ hybridization. DLL3 RNA expression is detected in SCLC tumor, SHP-77 SCLC cell line and normal pituitaries, but not other normal tissues. Red dots represent positive staining. Expression was given a semi-quantitative visual score (RNA score) of 0-4. (**E**) Quantification of DLL3 surface protein in SCLC cell lines and PDX models suggest most cell lines and PDX models express lower than 2000 copies of surface DLL3 molecules. Numbers in the graph indicate DLL3 surface copy number.

Fig. S2

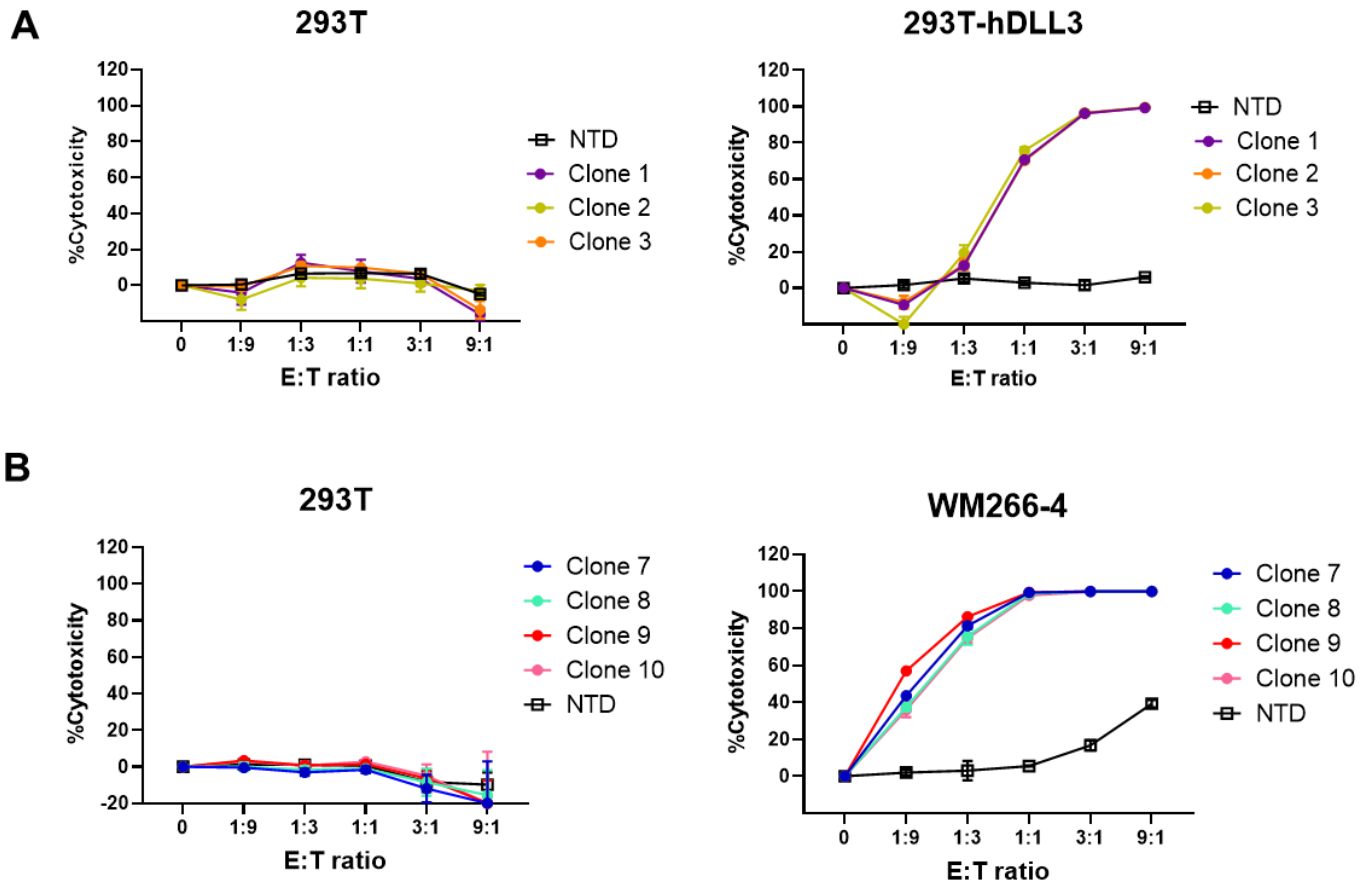

Fig. S2. DLL3 CAR T cells demonstrate specific cytotoxicity against DLL3-positive but not DLL3-negative targets. (**A**) Clones 1, 2 and 3 showed cytotoxicity against 293T cells expressing exogenous human DLL3 (293-hDLL3) but not against DLL3-negative parental 293T cells. DLL3 CAR cells and target cells were co-cultured for 72 hours and viability was measured using ONE-Glo assay system (Promega). Results represent mean ± SD, n=3. (**B**) Clones 7, 8 ,9 and 10 showed cytotoxicity against DLL3-positive WM266.4 cells but not against DLL3-negative parental 293T cells. Results represent mean ± SD, n=3 technical replicates.

Fig. S3

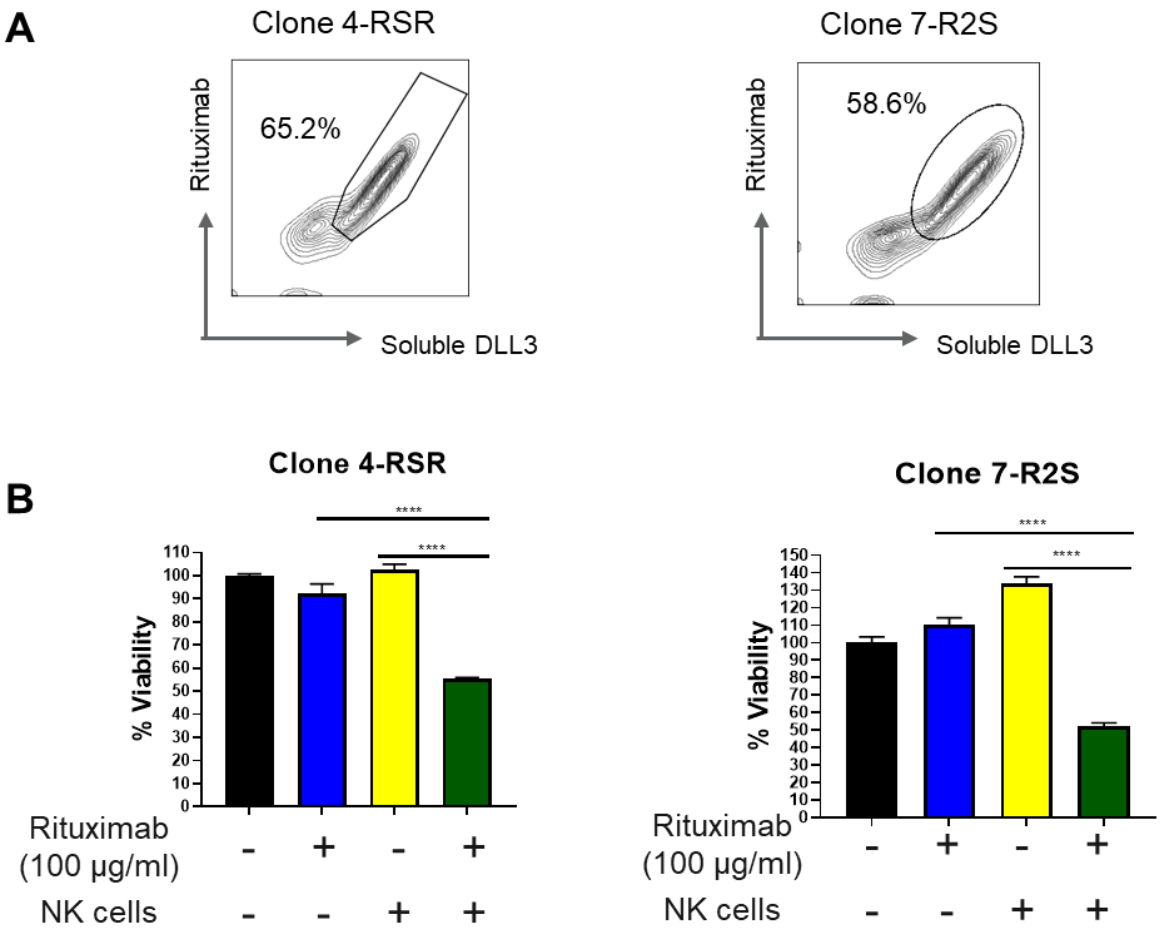

Fig. S3. DLL3 CAR T cells with rituximab off-switch can be detected by rituximab and eliminated by ADCC. (**A**) T cells transduced with clone 4-RSR or clone 7-R2S can be detected by co-staining of rituximab and soluble DLL3. (**B**) T cells transduced with clone 4-RSR or clone 7-R2S were depleted in antibody-dependent cellular cytotoxicity (ADCC) assay. NK cells were purified from PBMCs and activated with 1000 IU/ml IL-2 for 3 days and then incubated with freshly thawed CAR T cells for 24 hours with or without rituximab (100 µg/ml). Live CAR+ cells were counted on flow cytometer at the end of the assay. Groups were analyzed by using One Way ANOVA with Tukey's correction for multiple comparisons (****,$p<0.0001$, n=3). Error bars represent SEM.

Fig. S4

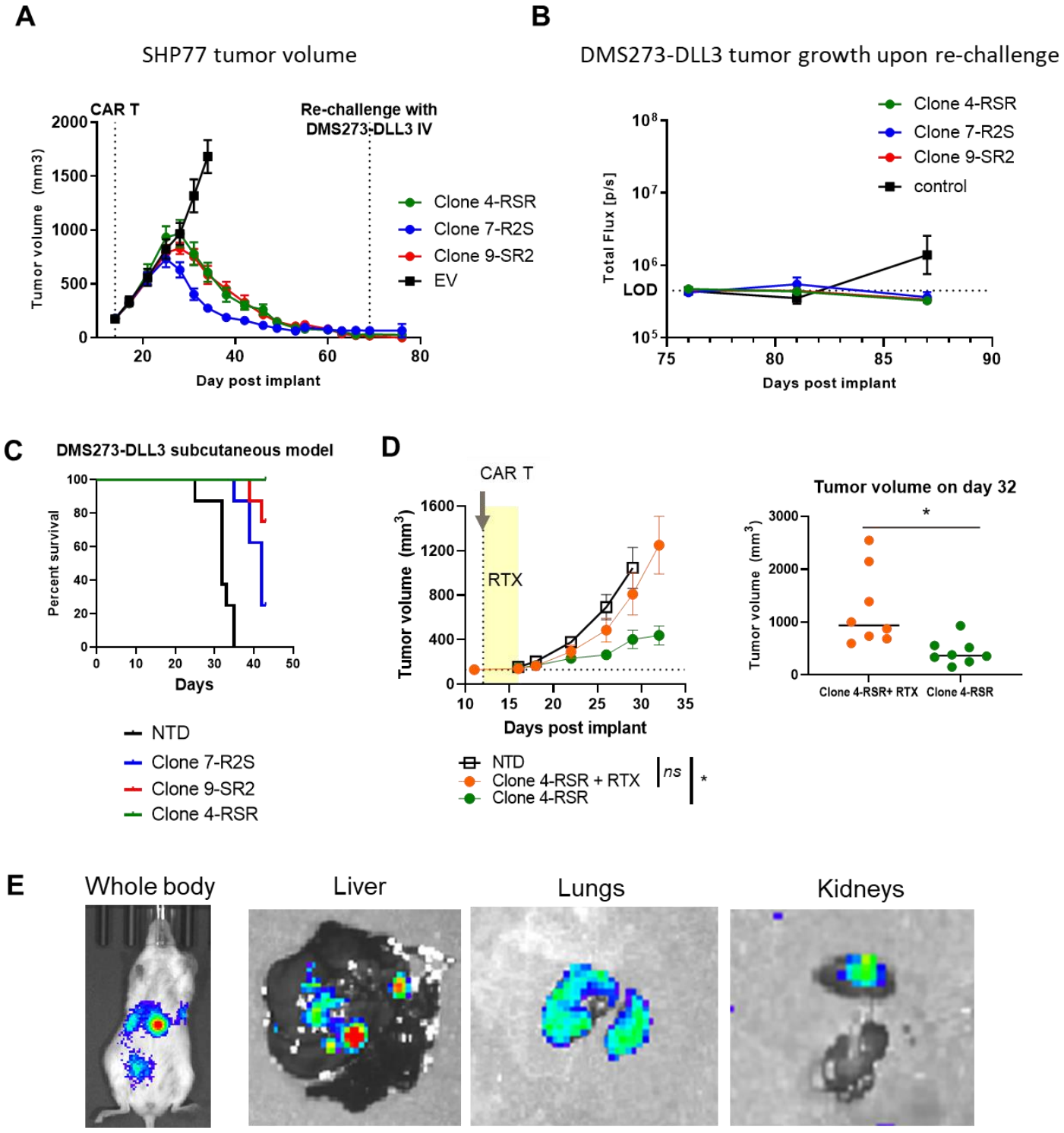
A
SHP77 tumor volume
CAR T
Re-challenge with DMS273-DLL3 IV
Tumor volume (mm3)
Day post implant
Clone 4-RSR
Clone 7-R2S
Clone 9-SR2
EV
B
DMS273-DLL3 tumor growth upon re-challenge
Total Flux [p/s]
LOD
Days post implant
Clone 4-RSR
Clone 7-R2S
Clone 9-SR2
control
C
DMS273-DLL3 subcutaneous model
Percent survival
Days
NTD
Clone 7-R2S
Clone 9-SR2
Clone 4-RSR
D
CAR T
RTX
Tumor volume (mm3)
Days post implant
NTD
Clone 4-RSR + RTX
Clone 4-RSR
ns
*
Tumor volume on day 32
Tumor volume (mm3)
Clone 4-RSR+ RTX
Clone 4-RSR
E
Whole body
Liver
Lungs
Kidneys

Fig. S4 continued

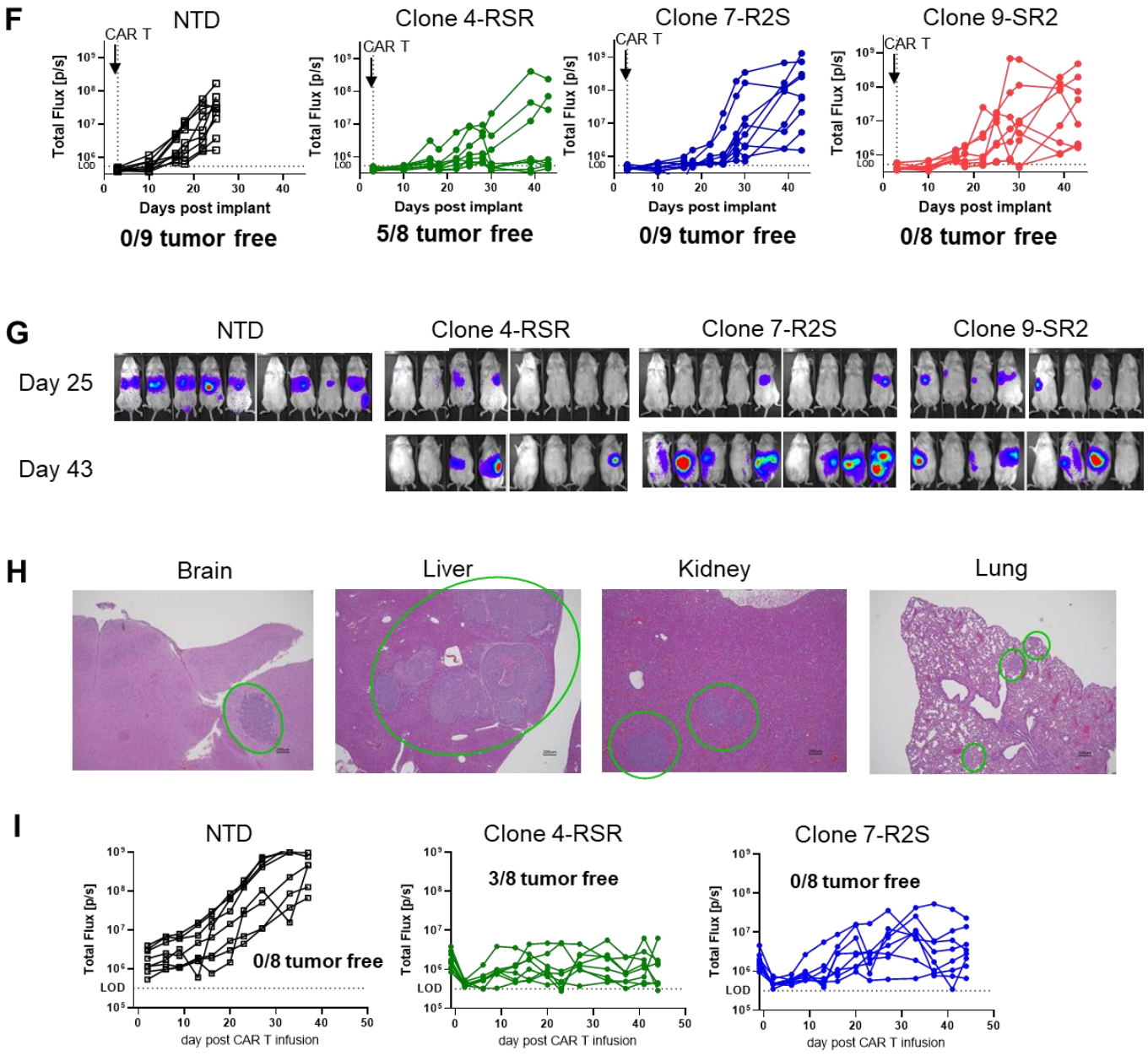

Fig. S4. In vivo activity of DLL3 CAR T cells. (**A**) The study shown in Fig. 4A was monitored for tumor growth out to 87 days. Most mice remained tumor free of SHP77 SC tumors and were re-challenge with luciferase-labeled DMS273-DLL3 tumors injected intravenously at $1x10^5$ cells/mouse on day 69. (**B**) The DMS273-DLL3 tumor burden in the study shown in Fig. S4A

was tracked by luminesce imaging and compared to tumor burden in naïve non-CAR treated mice. No detectable tumor was observed in DLL3 CAR-treated mice, while tumors did begin to grow out in CAR naïve control mice. (**C**) Survival curve of DMS273-DLL3 subcutaneous model demonstrating that animals who received clone 4-RSR had the best survival at the end of the study. (**D**) Rituximab treatment efficiently suppressed in vivo activity of DLL3 CAR T cells. DMS273-DLL3 cells were implanted subcutaneously and a single dose of CAR T cells ($3x10^6$ CAR+ cells per animal) were injected on day 12. Starting from the day of CAR T dosing, 10 mg/kg rituximab (RTX) was dosed for 5 consecutive days via IP injection. RM One Way ANOVA was performed on tumor volume on days 16-29 with Dunnett's multiple comparisons test, $p<0.05$. Paired t-test was performed on tumor volume on day 32. *, $p < 0.05$. Error bars represent SEM, n=8. (**E**) Representative bioluminescence image of mouse, liver, lungs, and kidneys after IV implantation of DMS273-DLL3 tumor cells. (**F**) Tumor burden of individual animals in DMS273-DLL3 systemic model demonstrating only the clone 4-RSR-treated group had tumor-free animals. (**G**) Bioluminescence images of animals in DMS273-DLL3 systemic model. (**H**) H&E images demonstrating tumor cells in SHP-77 systemic model were detected in brain, liver, kidney and lung. Green circles indicate tumor cells. (**I**) Tumor burden of individual animals in SHP-77 systemic model demonstrating only clone 4-RSR-treated group had tumor-free animals.

Fig. S5

A

		Clone 9	Clone 4	Clone 7
Positive Cell Pellet		Staining	Staining	Staining
Epithelium	Esophageal and salivary gland (cytoplasm)	1-2+ (occas)	No staining	No staining
	Testis (***membrane*** & cytoplasm)	No staining	***1-3+ (rare to occas)***	No staining
	Pancreas, skin, tonsil, anterior pituitary (cytoplasm)	No staining	1-3+ (rare to occas)	No staining
Myoepithelium	Mammary gland (cytoplasm)	1-3+ (freq)	No staining	No staining
Mononuclear cells	Esophagus, pancreas, pituitary (interstitium), and tonsil (***membrane*** & cytoplasm)	***1-3+ (rare to occas)***	No staining	No staining
Reticular cells and fibers	Lymph node and spleen (***membrane*** & cytoplasm)	***2-4+ (freq)***	No staining	No staining
Vascular and/or intrinsic smooth myocytes	> 30 human tissues (cytoplasm)	1-4+ (occas to freq)	No staining	No staining
Adipocytes	Pancreas (cytoplasm)	No staining	1-3+ (rare)	No staining

B

		Clone 4	Clone 7
Positive Cell Pellet		Staining	Staining
Negative Cell Pellet		No Staining	No Staining
Epithelium	**Pancreas, acini and duct (membrane & cytoplasm)**	**1-3+ (occas), all 3 donors**	No staining
	Testis, Spermatogenic cells (membrane & cytoplasm)	1-3+ (rare to freq), all 3 donors	No staining
Amnion	Placenta (membrane & cytoplasmic)	1-3+ (freq), 1 of 3 donors	No staining

C

		Clone 4(Lot 1)	Clone 4(Lot 2)
Positive Cell Pellet		Staining	Staining
Negative Cell Pellet		No Staining	No Staining
Pancreas	**Membrane staining**	**No staining (all 8 donors)**	**No staining (all 8 donors)**
	Extracellular material in duct and acinar lumina	1-3+, rare (1 of 8 donors)	1-3+, rare (1 of 8 donors)
	Cytoplasm of duct epithelial cells	No staining	1+, rare (1 of 8 donors)

For panels A-C, 1+ = weak, 2+ = moderate, 3+ = strong, 4+ = intense, occas = occasional, freq = frequent. Frequency modifiers were included to provide the approximate percentage staining of expected numbers of that cell type or tissue element at that location. The frequency of cells with staining was identified as follows: very rare (<1% of cells of a particular cell type); rare (1-5% of cells of a particular cell type); rare to occasional (>5-25% of cells of a particular cell type); occasional (>25-50% of cells of a particular type); occasional to frequent (>50-75% of cells of a particular cell type); frequent (>75-100% of cells of a particular cell type).

Fig. S5 continued

D

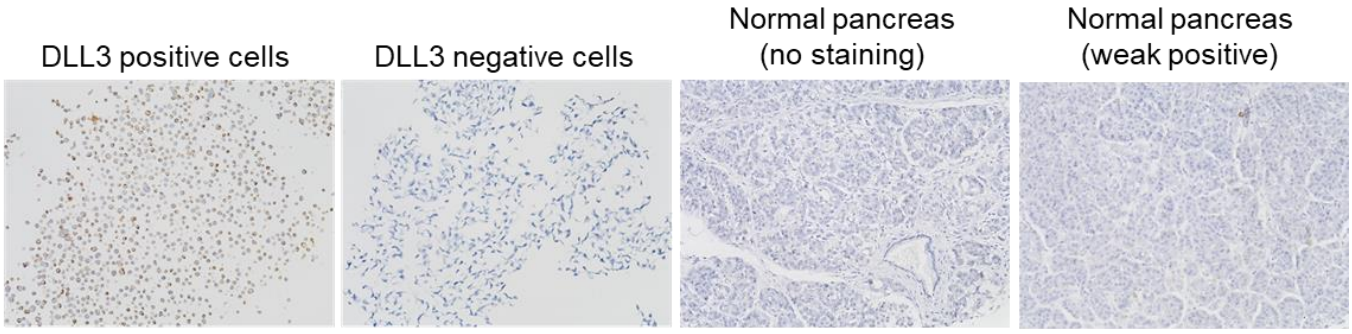

E

Normal pancreatic tissue (N=20)	**N=16**	**No staining**
	N=2	Equivocal positive staining (cytoplasmic), rare
	N=2	Weak positive staining (cytoplasmic), rare

F

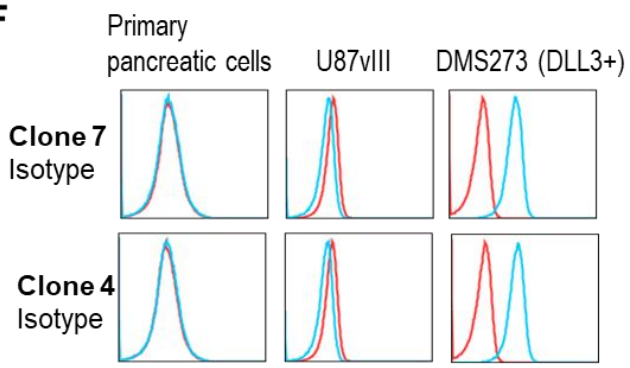

G

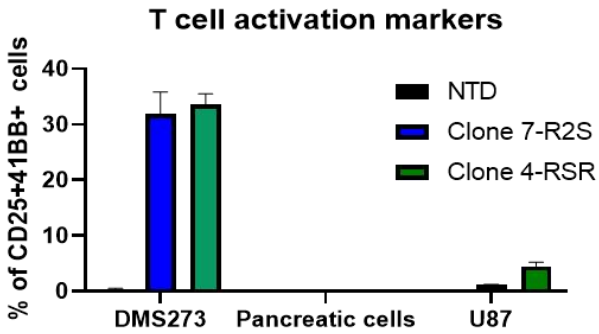

H

	Age matched control (n=3)	Clone 4-RSR (n=5)
Infiltration	No infiltration	Minimal (n=1) Mild (n=1)
Decreased secretory material (acinar cell)	No findings	Minimal (n=1) Mild (n=4)

Fig. S5. Clone 4 showed pancreatic membrane staining in one of three TCR studies but other derisking studies suggest the staining may be artifactual. (**A**) Clone 9 showed off-target binding to multiple tissues in initial TCR study and was eliminated as a candidate. The scFv binding domains of clone 4, 7 and 9 were fused to a human IgG2 Fc fragment and assayed using immunohistochemistry (IHC) against a panel of 36 human tissues to evaluate binding from 1 donor. Results are shown for staining at 10 mg/mL. DLL3-positive and negative cell pellets were utilized as controls. Staining was scored by a board-certified pathologist on both intensity and frequency. Scoring is shown for control cell pellets and for tissues in which positive staining with either CARs 9 or 4 was observed. (**B**) Membrane staining of clone 4 was observed in epithelial cells in the pancreas (acini, ducts), amnion in the placenta and spermatogenic cells in the testis. The scFv binding domains of clone 4 and 7 were tested using methods described in (A) against a panel of 36 human tissues to evaluate binding from 3 donors. Results are shown for staining at 10 μg/mL. Scoring is shown for control cell pellets and for tissues in which membrane staining with clone 4 was observed. (**C**) Follow-up study to further evaluate pancreatic membrane staining was performed using the same protocol with 8 additional human donors and two lots of clone 4 soluble binding domain. No pancreatic membrane staining was observed in any donors. (**D**) Additional IHC work was performed in-house and no pancreatic membrane staining was observed. Representative images of clone 4 staining on DLL3-positive cells, DLL3-negative cells and 2 normal pancreas samples were shown. (**E**) In-house IHC staining of 20 normal pancreas samples (US Biomax) was reviewed by a pathologist. Staining pattern and intensity was summarized in the table. (**F**) Clone 4 and clone 7 showed binding to DLL3 positive DMS273 cells but not to human primary pancreatic cells. Data from one representative donor is shown. (**G**) Clone 4 and clone 7 CAR T cells are not activated after co-cultured with primary pancreatic cells for 2 days at an E:T of 2:1. Error bars represent standard deviation, n=4 technical replicates. Experiments were performed 3 times with DLL3 CAR Ts generated from different donors. Data from one representative donor is shown. (**H**) DLL3 CAR T cells-related changes in pancreas are limited to minimal/mild zymogen decrease and lymphocyte infiltrates. Animals bearing SHP-77 subcutaneous tumors received a single dose of NTD or DLL3 CAR T cells ($5x10^6$ CAR+ per animal). After tumor clearance, pancreas tissues were collected, H&E stained and analyzed by a pathologist.

Fig. S6

A

Sample	Section	DLL3 RNA score	% Positive	Comments
Animal 1	1	1	<10%	
	2	1	<10%	Subset of cells score 2
	3	1	<10%	Subset of cells score 2
	4	2	<10%	Localized in ventricular system
Animal 2	1	1	<10%	
	2	1	<10%	
	3	1	<10%	Subset of cells score 2
	4	2	<10%	Localized in ventricular system
Animal 3	1	1	<10%	
	2	1	<10%	
	3	2	<10%	
	4	2	<10%	

Animal#1 Section 2

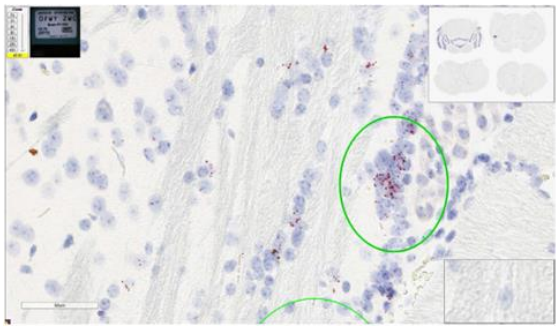

Green circle: subset of cells score 2

RNA score 0 = No staining or <1 RNA molecule / 10 cells, 1 = 1-3 RNA molecules/cell , 2 = 4-9 RNA molecules/cell, no or very few dot clusters, 3 = 10-15 RNA molecules/cell and/or <10% dots are in clusters, 4 = >15 RNA molecules/cell and/or >10% dots are in clusters. Percentage of cells positive is scored visually based on number of cells with >1 dot/cell and binned into categories (i.e., 0%, 1-25%, 26-50%, 51-75%, 76-99%, 100%)

B

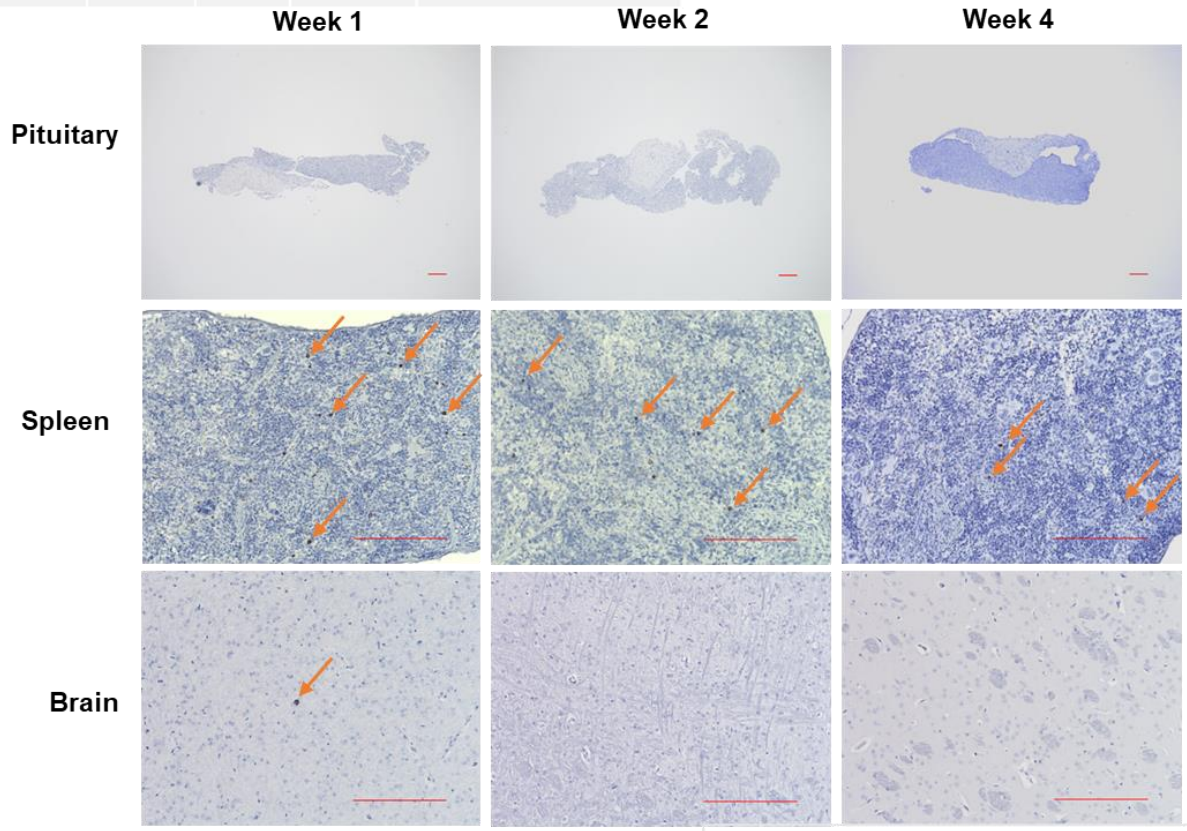

C

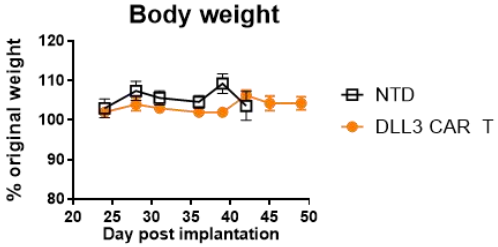

D

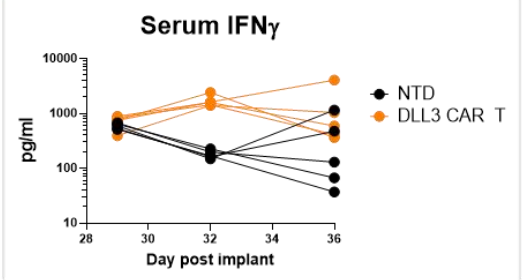

Fig. S6 continued

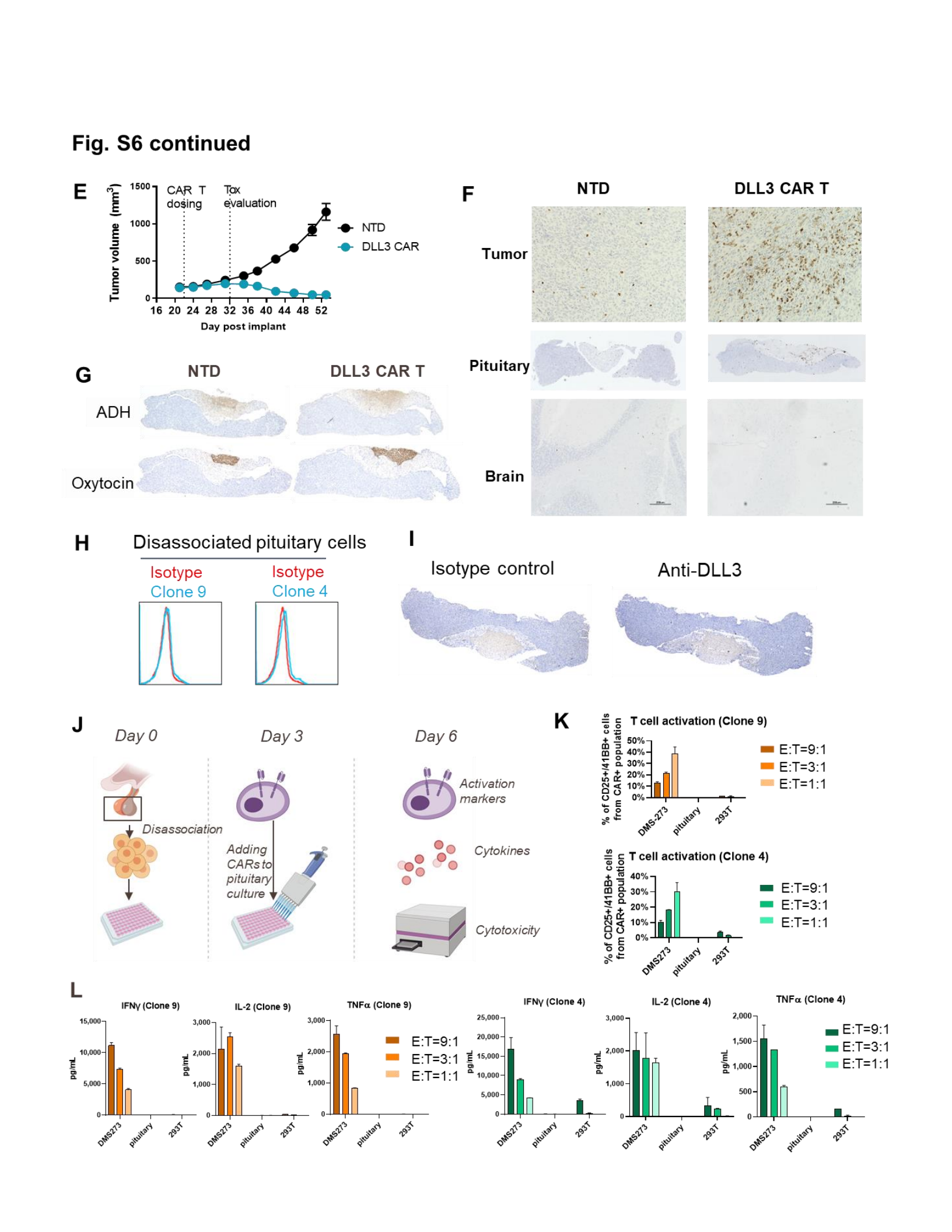

Fig. S6. Infusion of DLL3 CAR T cells did not induce toxicity in non-tumor-bearing model or subcutaneous tumor model. (**A**) Mouse brain tissues express DLL3 RNA. Brain tissues from three tumor-free and treatment-free NSG mice were harvested and used for single-color chromogenic RNAscope assay with mouse DLL3 specific probe. Discrete red dots corresponded to individual RNA targets. Visual scoring is performed by a qualified scientist to assign a single score to a sample based on the predominant staining pattern throughout the entire sample. (**B**) T cells were not detected in brain or pituitary samples from non-tumor bearing animals injected with a high dose ($8X10^6$) of NTD or DLL3 CAR T cells. Tissues were collected 1, 2, or 4 weeks post T cell injection. Scale bars represent 200 μm. Orange arrows point to T cells in the tissues. (**C**) DLL3 CAR T cells did not induce obvious changes of body weight throughout the study. (**D**) Serum was collected from animals treated with NTD or DLL3 CAR T cells on day 29, 32 and 36 post T cell infusion and analyzed using meso-scale discovery (MSD) to measure cytokines. Serum collected on day 32 from DLL3 CAR T treated animals has the highest levels of IFNγ. (**E**) NTD or DLL3 CAR T cells were injected into animals bearing LN229-mDLL3 subcutaneous tumors. A subset of animals were euthanized on day 32 (time of peak of CAR T activity) post CAR T infusion to analyze T cell infiltration into tumor, pituitary and brain. Error bars represent SEM, n=5. (**F**) IHC study using anti-human CD45 antibody revealed dense infiltration into subcutaneous tumor and sparse infiltration into pituitary tissues. (**G**) Despite low levels of T cell infiltration into pituitary tissues, pituitary hormones (ADH and oxytocin) can still be detected using IHC, suggesting hormone-secreting function of pituitary was not affected. (**H**) Surface DLL3 protein was not detected on disassociated mouse pituitary cells using flow cytometry. Disassociated mouse pituitary cells were stained with 2ug/ml of clone 4, clone 9 or isotype control antibody followed by anti-human IgG secondary antibody conjugated with PE. (**I**) DLL3 protein was not detected in mouse pituitary samples using IHC. (**J**) Design of in vitro cytotoxicity study (**K**) Surface staining for CD25 and 41BB of DLL3 CAR T cells co-cultured with targets for 3 days, demonstrating that mouse pituitary cells do not activate DLL3 CAR Ts. Error bars represent standard deviation, n=3. (**L**) DLL3 CAR Ts do not secret cytokines when co-cultured with mouse pituitary cells. Error bars represent standard deviation, n=3.

Fig. S7

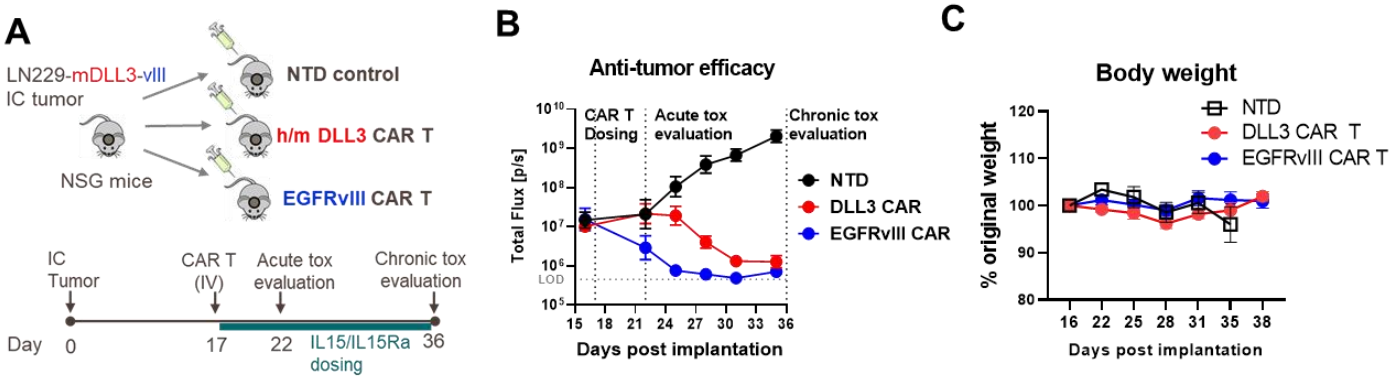

D Histopathology Analysis

Group	Acute tox evaluation (day 22)			Chronic tox evaluation (day 36)		
	Animal	Brain	Pituitary	Animal	Brain	Pituitary
NTD	#1	Tumor	No findings	#3	No findings	No findings
	#2	No findings	No findings	#4	Tumor	No findings
	#5	No findings	No findings	#7	Tumor	No findings
	#6	No findings	No findings	#8	Tumor	No findings
	#10	No findings	No findings	#9	Tumor	No findings
DLL3 CAR T	#12	Tumor	No findings	#11	Tumor	Infiltrate, mononuclear cell (Grade 2)
	#14	Tumor	No findings	#13	Tumor	Infiltrate, mononuclear cell (Grade 2)
	#15	Tumor	No findings	#16	Tumor	Infiltrate, mononuclear cell (Grade 1)
	#19	No findings	No findings	#17	No findings	Infiltrate, mononuclear cell (Grade 2)
	#20	Tumor	No findings	#18	No findings	Infiltrate, mononuclear cell (Grade 2)
EGFRvIII CAR T	#22	No findings	No findings	#21	No findings	No findings
	#25	Infiltrate/gliosis, cortical, focal (Grade 2)	No findings	#27	No findings	No findings
	#26	Infiltrate, meninges, focal (Grade 1)	No findings	#29	No findings	No findings
	#31	Infiltrate/gliosis, cortical, focal (Grade 2)	No findings	#30	No findings	No findings
	#32	Gliosis/infiltrate, cortical, focal (Grade 1)	NA	#35	No findings	No findings

**Severity: Grade 1=Minimal; Grade 2=Mild; Grade 3=Moderate

E

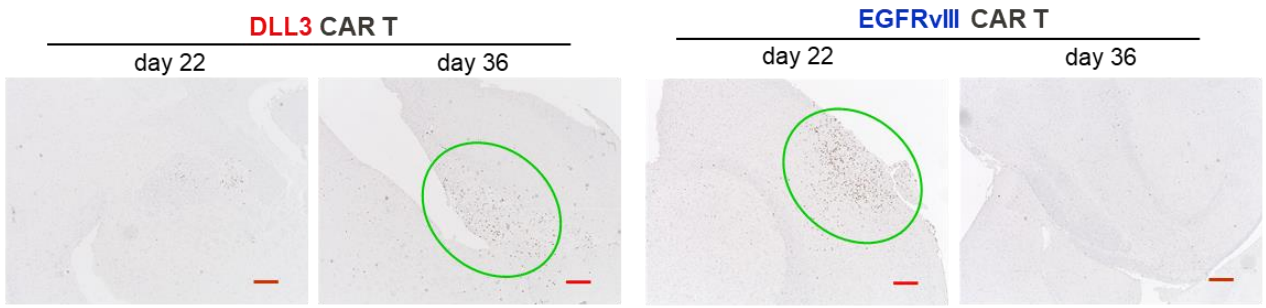

F Staining of pituitary hormones (day 36)

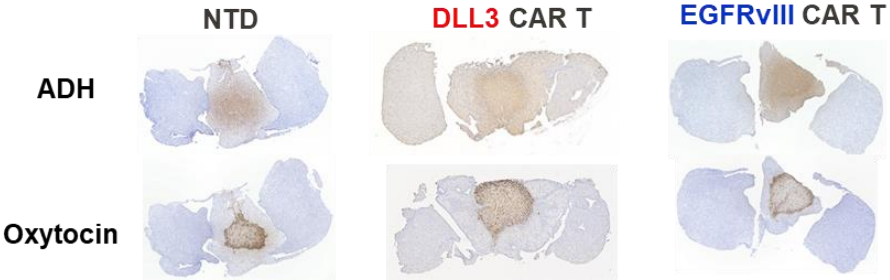

Fig. S7. DLL3 CAR T cells demonstrate activity in intracranial tumor model without causing toxicity. (**A**) & (**B**) Design and anti-tumor efficacy of in vivo study with intracranial tumor expressing DLL3 and EGFRvIII to understand tox liabilities. LOD, limit of detection. Plots represent only the animals remaining on D36 (n=5). Error bars represent SEM. (**C**) DLL3 CAR T cells or EGFRvIII CAR T cells did not induce obvious changes of body weight throughout the study. Plots represent only the animals remaining on D36 (n=5). Error bars represent SEM. (**D**) Histopathology analysis showed mild infiltration/inflammation in pituitary of DLL3 CAR-treated animals. No findings for brain samples. (**E**) Infiltration of DLL3 CAR T and EGFRvIII CAR T cells in the area of glioma in the brain. Green circles show the area of infiltration. (**F**) Hormone secreting cells were not ablated despite T cell infiltration.